

**THE SHROOM FAMILY MEMBER, APXL, BINDS ACTIN AND LOCALIZES TO  
SITES OF CELL ADHESION**

By

Jennifer E. Phillips

BA, William Smith College, 1999

Submitted to the Graduate Faculty of  
Arts and Sciences in partial fulfillment  
of the requirements for the degree of  
Master of Science

University of Pittsburgh

2006

UNIVERSITY OF PITTSBURGH  
FACULTY OF ARTS AND SCIENCES

This thesis was presented

by

Jennifer E. Phillips

It was defended on

[Month date, year]

and approved by

Jeffrey Brodsky, PhD, Associate Professor, Department of Biological Sciences

Beth Stronach, PhD, Assistant Professor, Department of Biological Sciences

Kirill Kiselyov, PhD, Assistant Professor, Department of Biological Sciences

Thesis Director: Jeffrey Hildebrand, PhD, Associate Professor, Department of Biological Sciences

# **THE SHROOM FAMILY MEMBER, APXL, BINDS ACTIN AND LOCALIZES TO SITES OF CELL ADHESION**

Jennifer E. Phillips, M.S.

University of Pittsburgh, 2006

The actin cytoskeleton is essential for a vast array of cellular processes and behaviors including migration, cell adhesion, intracellular trafficking, and maintenance of cell shape. Regulation of cytoskeletal dynamics is achieved through the actions of a diverse group actin-binding proteins. The actin-binding protein Apxl, is a member of the Shroom protein family, which also includes Apx and KIAA1202. Shroom, the most well-characterized member of this family, binds and bundles actin stress fibers and is required for apical constriction of the neuroepithelium during neural tube closure in mice and *Xenopus* embryos. Apxl was named for its similarity to Apical Protein Xenopus (Apx), a regulator of an amiloride-sensitive sodium channel. All Shrm family members possess at least two of three conserved domains; a N-terminal PDZ domain, a centrally located ASD1 (APX/Shroom Domain) and a C-terminal ASD2 domain. Because of its similarity to Shroom, mouse Apxl was sequenced and cloned in order to begin initial characterization of the protein. Western blot analysis has shown that mApxl is expressed in the majority of adult tissues. Immunofluorescence analysis of frozen sections has demonstrated that Apxl is specifically expressed in multiple populations of polarized cells, such as the neuroepithelium, vascular endothelium, and the epithelium of renal tubules. The subcellular localization of Apxl was investigated and Apxl was found to reside at the plasma membrane of non-adherent cells and in the apical compartment of polarized cells, possibly through interactions with cortical actin or members of the apical junctional complex. Analysis of Apxl deletion proteins has revealed that the ASD1 domain is crucial for proper localization, while the requirement for the PDZ

domain varies in different cell lines. Cytochalasin D treatment of Rat1 fibroblasts has indicated that disruption of the actin cytoskeleton perturbs Apxl localization. Additionally, Apxl directly binds actin through its ASD1 domain in F-actin cosedimentation experiments. Apxl is expressed in multiple polarized cell types where it binds cortical actin and localizes to the apical junctional complex. Although the biological function of Apxl is unknown, its expression pattern, subcellular localization, and similarity to Shroom suggest that Apxl plays a role in regulation of cellular architecture throughout development.

## TABLE OF CONTENTS

<b>PREFACE.....</b>	<b>VIII</b>
<b>1.0 INTRODUCTION.....</b>	<b>1</b>
<b>1.1 ACTIN-BINDING PROTEINS AND CELL BEHAVIOR.....</b>	<b>1</b>
<b>1.2 CELL POLARITY AND INTERCELLULAR ADHESIONS .....</b>	<b>3</b>
<b>1.3 THE SHROOM PROTEIN FAMILY .....</b>	<b>4</b>
<b>1.4 NEURAL TUBE DEFECTS AND NEURAL TUBE CLOSURE .....</b>	<b>7</b>
<b>1.5 THE ROLE OF SHROOM IN NEURAL TUBE CLOSURE .....</b>	<b>11</b>
<b>1.6 THESIS OVERVIEW .....</b>	<b>12</b>
<b>2.0 MATERIALS AND METHODS .....</b>	<b>13</b>
<b>2.1 CELL CULTURE.....</b>	<b>13</b>
<b>2.2 MOLECULAR BIOLOGY.....</b>	<b>13</b>
<b>2.3 ANTIBODIES, WESTERN BLOTTING AND IMMUNOFLUORESCENCE .</b> .....	<b>14</b>
<b>2.4 CO-IMMUNOPRECIPITATION.....</b>	<b>16</b>
<b>2.5 ACTIN BINDING.....</b>	<b>16</b>
<b>3.0 EXPRESSION PROFILE OF APXL .....</b>	<b>17</b>
<b>3.1 RESULTS.....</b>	<b>17</b>
<b>3.2 DISCUSSION.....</b>	<b>22</b>

<b>4.0</b>	<b>APXL LOCALIZES TO SITES OF CELL ADHESION.....</b>	<b>25</b>
<b>4.1</b>	<b>RESULTS .....</b>	<b>25</b>
<b>4.1.1</b>	<b>Immunoprecipitation and Immunofluorescence.....</b>	<b>25</b>
<b>4.1.2</b>	<b>Apxl Deletion Constructs .....</b>	<b>29</b>
<b>4.1.3</b>	<b>Apxl binds actin but does not cause apical constriction.....</b>	<b>34</b>
<b>4.2</b>	<b>DISCUSSION.....</b>	<b>37</b>
<b>5.0</b>	<b>SUMMARY AND CONCLUSIONS .....</b>	<b>41</b>
	<b>BIBLIOGRAPHY.....</b>	<b>43</b>

## LIST OF FIGURES

Figure 1: Components of the intercellular junctional complex .....	4
Figure 2: The Shroom protein family .....	7
Figure 3: Morphogenetic movements during neural tube closure .....	9
Figure 4: The purse-string model of apical constriction.....	10
Figure 5: Apxl is widely expressed in adult tissue lysates.....	18
Figure 6: Apxl localizes to the apical surface of neural epithelium and to dorsal root ganglia....	20
Figure 7: Apxl is expressed in renal collecting ducts .....	21
Figure 8: Apxl is expressed in adult intestine.....	22
Figure 9: Apxl localizes to cell adhesions .....	26
Figure 10: Apxl localizes to tight junctions in MDCK cells .....	27
Figure 11: Apxl co-immunoprecipitation experiments.....	28
Figure 12: Apxl deletion constructs.....	31
Figure 13: Localization of Apxl truncation proteins varies with cell type .....	34
Figure 14: Apxl localization collapses after cytochalasin treatment .....	35
Figure 15: Apxl localizes to cortical actin but not to stress fibers.....	36
Figure 16: Summary of Apxl localization .....	38

## PREFACE

I would like to thank my thesis advisor, Dr. Jeffrey Hildebrand, for giving me the opportunity to join his laboratory, and for the mentoring and guidance he provided. I would like to thank my committee, Dr. Jeffrey Brodsky, Dr. Beth Stronach, and Dr. Kirill Kiselyov for their time.

I would also like to thank the entire Hildebrand lab, past and present, for providing an enjoyable working environment, especially Mick Yoder, for assistance and advice. I would like to acknowledge Frank Vendetti and Teresa Bernaciak for their work on the F-actin cosedimentation experiments and for assistance in creating the *Apxl* deletion constructs.

Finally, I would also like to thank all of my friends in the department, including Stacy Hrizo and Alycia Bittner, for all of their advice and support. Most of all, I am grateful for all the understanding and support I have received from my family, especially my husband, Tom, my parents, and my brothers.

## **1.0 INTRODUCTION**

### **1.1 ACTIN-BINDING PROTEINS AND CELL BEHAVIOR**

The complex process of cell and tissue movements that culminate in a highly organized embryo is one of the most fascinating aspects of developmental biology. These dramatic morphogenetic movements are crucially dependent upon the actin cytoskeleton. Indeed, eukaryotic cells depend upon their actin cytoskeleton for a wide array of processes and behaviors. The actin cytoskeleton is essential for activities such as migration, cell division, cell/cell and cell/substratum adhesion, and intracellular trafficking [1-7]. Additionally, the development, maintenance, and alteration of cell structure and shape are dependent upon the actin cytoskeleton. Regulation of cytoskeletal dynamics is controlled by a diverse group of proteins referred to as actin-binding proteins (ABPs). Several different classes of ABPs exist that regulate functions such as G-actin sequestration, actin assembly/disassembly, filament severing or capping, crosslinking, and bundling proteins. Other known ABPs function as adaptor proteins to link actin to other cytoskeletal elements or to the plasma membrane [3, 5, 8].

Cellular motility is dependent upon biomechanical forces generated by the actin cytoskeleton and associated proteins [4, 9, 10]. Migration can be visualized as a cyclical process. In the first step, actin-polymerization drives the extension of a wide, sheet-like lamellipodium or a narrow, finger-shaped filopodium [4, 10]. The extended cellular protrusion anchors the cell to

the extracellular matrix via focal contacts. Subsequently, contraction of actomyosin filaments provides the traction force required to pull the cell forward and to induce disassembly of focal contacts at the rear of the cell [2, 10]. ABPs play a role in cell migration by regulating the architecture of the protrusion. N-WASP proteins and the Arp2/3 complex are known to regulate lamellipodium formation by nucleating new actin filaments. Similarly, Ena/VASP family proteins play a role in regulating the growth of filopodia. Numerous other ABPs determine the rate of actin polymerization, and hence influence the rate of migration, by regulating the availability of G-actin monomers and free ends [2, 4, 5]. For example, ADF/cofilin family proteins enhance the pool of actin monomers by promoting filament severing and disassociation.

The actin cytoskeleton and associated ABPs are also intimately involved in the establishment, maintenance and rearrangement of cell-cell and cell-matrix adhesions. Indeed, cell contacts such as focal adhesions or adherens junctions (AJ) function to link the actin cytoskeleton to the extracellular matrix or to the cytoskeleton of neighboring cells. Formation of cell adhesions and organization of the actin cytoskeleton are interdependent processes. For example, disruption of the *Drosophila* Armadillo, a homolog of vertebrate  $\beta$ -catenin, leads to widespread polarity defects in the actin cytoskeleton [1]. Conversely, depolymerization of cortical actin disrupts AJs [11]. However, the role of the actin cytoskeleton in AJ formation is not simply to act as a scaffold to cluster cadherins at the plasma membrane. Although cadherin proteins bind preformed actin filaments, interactions between cadherins and the Arp2/3 complex play a role in the establishment of AJs by regulating actin polymerization at sites of cell-cell contact [12, 13].

## 1.2 CELL POLARITY AND INTERCELLULAR ADHESIONS

Apical-Basal polarity is a fundamental aspect of epithelial cells and is an essential requirement for many of their processes and functions, including vectorial transport, signal transduction, cell adhesion, and barrier formation. Polarized cells are generally understood as possessing three membrane domains, the apical, lateral, and basal. Tight junctions (TJ) form the most apical component of the junctional complex and define the border between the apical and lateral membranes (Fig. 1). Tight junctions function mechanically as a barrier to epithelial permeability and as a fence to restrict the movement of membrane proteins and lipids between the apical and basal/lateral compartments [14]. Occludin, claudins, and junctional adhesion molecule (JAM) constitute the integral membrane proteins of the tight junctions [15-17]. Numerous accessory and regulatory proteins localize to the cytoplasmic plaque of tight junctions, such as ZO-1, -2, and -3, and Cingulin (Fig. 1).

The lateral membrane is defined by cell-cell adhesion complexes, such as adherens junctions and hemidesmosomes. AJs created cell-cell contacts through the homophilic binding of cadherins and link to the actin cytoskeleton through accessory proteins such as  $\alpha$ - and  $\beta$ -catenin and vinculin/ $\alpha$ -actinin (Fig. 1). Not only do AJs help to provide structural integrity for the cell, recent evidence suggests that cell-cell contacts are a crucial event in developing apical-basal polarity [18, 19]. Within the basal membrane cells are anchored to the extracellular matrix by focal adhesions and hemidesmosomes. These basal junctions provide mechanical strength by linking integrins to intermediate filaments at hemidesmosomes and to actin at focal adhesions.

Endothelial cells constitute another example of polarized cells and possess similar junctional organization. Both endothelial and epithelial cell types utilize adherens junctions and

tight junctions to join cells together. Major differences between these cell types include the absence of hemidesmosomes in endothelial cells [20-22]. Additionally, endothelial junctions are not as well organized and adherens junctions and tight junctions are often intermingled within the lateral membrane [20-22].

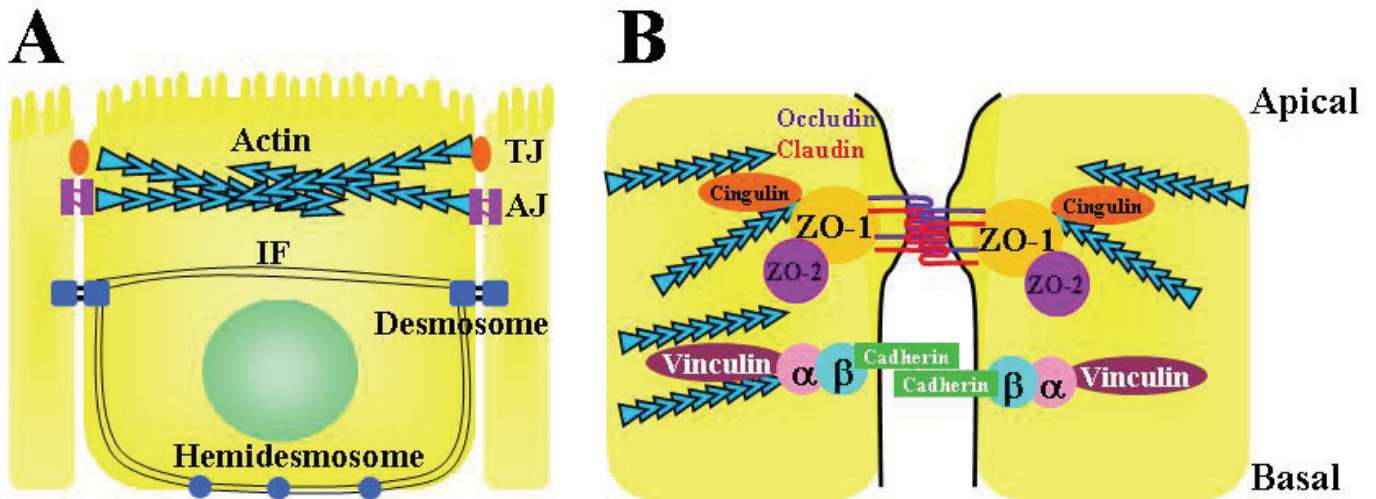


**Figure 1: Components of the intercellular junctional complex**

(A) Schematic of a typical mammalian epithelial cell with distinct apical and basolateral membrane domains, as well as specialized adhesion complexes such as tight junctions, adherens junctions, desmosomes and hemidesmosomes (IF = Intermediate filaments). (B) An enlarged view of the junctional complex highlighting some of the key components of tight junctions and adherens junctions.

### 1.3 THE SHROOM PROTEIN FAMILY

Shroom (Shrm) is an F-actin binding protein which is required for proper neural tube closure in mice and frogs [23, 24]. Shrm-deficient embryos display both exencephaly and spina bifida [23, 24]. Sequence analysis has revealed that *Shrm* is a member of a larger gene family which

includes the vertebrate proteins *apx* (Apical Protein Xenopus), *APXL* (Apical Protein Xenopus-Like), and *hKIAA1202*. All Shrm family members possess at least two of three conserved domains; an N-terminal PDZ domain, a centrally located ASD1 (APX/Shroom Domain) and a C-terminal ASD2 domain (Fig.2). PDZ (PSD95/DLG/ZO-1) domains are conserved protein-protein interaction domains which appear to be important for organizing protein complexes at the plasma membrane [25]. The ASD domains are novel domains with no previously determined function. Previous work has shown that the Shrm ASD1 is required for F-actin binding and proper subcellular localization. The ASD2 domain of Shrm has been shown to be necessary and, under specific conditions, sufficient to induce apical constriction [23]

Human *APXL* was identified because of its association with the X-linked ocular albinism [26]. Although *APXL* lies in close proximity to the *OA1* gene on the X-chromosome, no evidence supports a direct role in ocular albinism. *Apxl* was named for its similarity to Apical Protein Xenopus (*Apx*). *Apx* was identified by expression cloning using an antibody to the apical surface of *Xenopus* epithelial cells [27, 28]. *Apx* is believed to be a regulator of ENaC, an amiloride-sensitive sodium channel that plays an important role in kidney function [28, 29].

The similarity between *Apxl* and *Shrm* raises the possibility that *Apxl* functions in neural tube closure or the regulation of cellular architecture. The mouse homolog of *Apxl* was cloned and sequenced, in order to begin characterization of the protein. Sequence analysis indicates that, like *Shrm*, *Apxl* possesses an N-terminal PDZ domain, a centrally located ASD1 domain and a C-terminal ASD2 domain. *Apxl* is 35% identical to *Shroom* over the length of the protein, with much higher identity in the PDZ, ASD1, and ASD2 domains (64%, 52%, and 60%, respectively) [30].

KIAA1202 possesses both an N-terminal PDZ domain and a C-terminal ASD2 domain. Like other Shrm family members, *mKiaa1202* is expressed widely in mouse embryonic and adult tissues ([31] and Yoder, unpublished data). Despite lacking the actin-binding ASD1 domain, KIAA1202 localizes to actin-rich structures in the cytoplasm ([30, 31]. When the actin polymerization inhibitor latrunculin B is used to disrupt the actin cytoskeleton of HeLa cells, KIAA1202 remains associated with F-actin remnants. Although no known function of KIAA1202 has been determined, an association between KIAA1202 and X-linked mental retardation has recently been discovered [31].

Additionally, several putative invertebrate Shrm orthologs have been identified in *Drosophila*, *Ciona intestinalis* (sea squirt), and *Strongylocentrotus purpuratus* (sea urchin). The *Drosophila* ortholog, CG8603, possesses an ADS2 domain but lacks the PDZ or ASD1 domains. CG8603 over-expression has been reported to extend the longevity of flies [32]. Recent research has shown that CG8603 localizes to the cortical actin cytoskeleton in Rat1 fibroblasts and Shrm-CG8603 chimeras possessing the CG8603 ASD2 domain are capable of inducing apical constriction in MDCK cells [30]. Analysis of *Ciona* (CiGC24a06) and sea urchin (GenBank accession XM-778480) genomes has revealed putative *Shrm* orthologs which possess both the PDZ and ASD2 domains [30, 32].

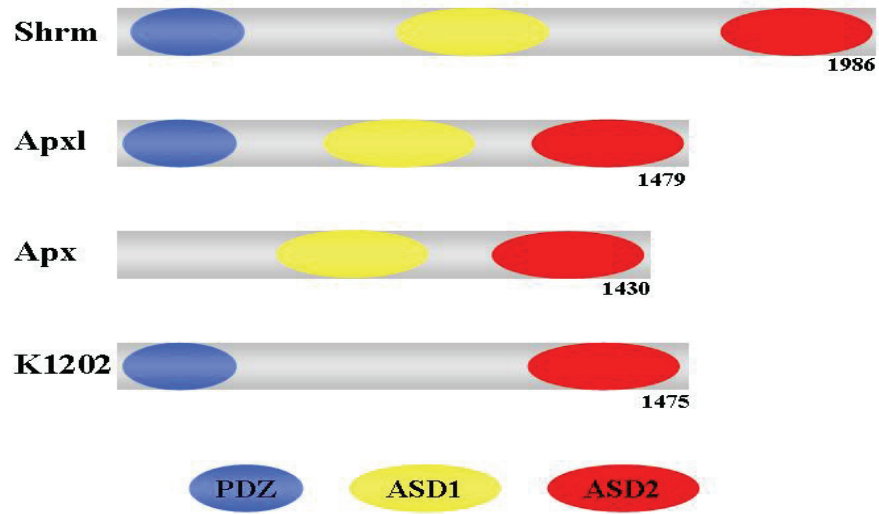


**Figure 2: The Shroom protein family**

The vertebrate members of the Shrm gene family include Shrm, Apxl, Apx and KIAA1202. Family members possess at least one of three conserved domains. The invertebrate family members are not pictured here.

#### 1.4 NEURAL TUBE DEFECTS AND NEURAL TUBE CLOSURE

Neural tube defects (NTDs) are a fairly common type of birth defect, affecting approximately 1 out of every 1000 live births [23, 33-36]. Failure of the neural tube to close properly results in serious birth defects such as anencephaly and spina bifida. Causes for NTDs are complex and multifactorial, involving both environmental and genetic influences. Although research has shown that a significant number of NTDs can be prevented by folic acid supplementation during

pregnancy, approximately 30% of NTDs remain resistant to folate supplementation [23, 37]. Misregulation of or mutations in numerous genes may result in NTDs and few single genetic defects are known to cause NTDs in humans. Over 80 mouse models for NTDs exist and indicate the importance of processes and pathways such as Shh signaling, convergent extension, apical constriction, and planar cell polarity in neural tube closure [23, 34, 35, 38-41]. Despite the clinical importance of neural tube closure, many of the molecular mechanisms regulating this morphogenetic process are still poorly understood.

Closure of the neural tube is a morphogenetic process in which a sheet of polarized epithelium, the neural plate, undergoes a series of morphogenetic movements driven by both internal and external forces. Briefly, neural tube closure occurs in three steps: the elevation of the neural plate, bending of the neural folds, and finally, fusion of the folds to form the neural tube [33, 42]. Once the neural plate has formed, it elongates along the rostral-caudal axis by convergent extension. Failure of planar cell polarity signaling and convergent extension leads to NTDs, presumably because the neural folds remain too far apart to appose and fuse [41, 43]. After elongation, the lateral borders of the neural plate elevate due, in part, to proliferative forces arising from underlying mesoderm [44]. Extrinsic forces, such as pushing forces generated by the surface ectoderm, also contribute to elevation of the neural folds [33, 42, 43]. Following elevation, bending of the neural folds occurs at specific sites referred to as hinge points. A medial hinge point (MHP) forms above the notochord, and two dorsolateral hinge points (DLHP) form on the lateral edges of the neural folds (Fig 3). This rotation of the neural folds around the hinge points allows their juxtaposition at the dorsal midline and fusion. Once the neural folds have fused to form a closed cylinder, differential expression of cell adhesion molecules cause the neural tube to separate from the surface ectoderm [45, 46].

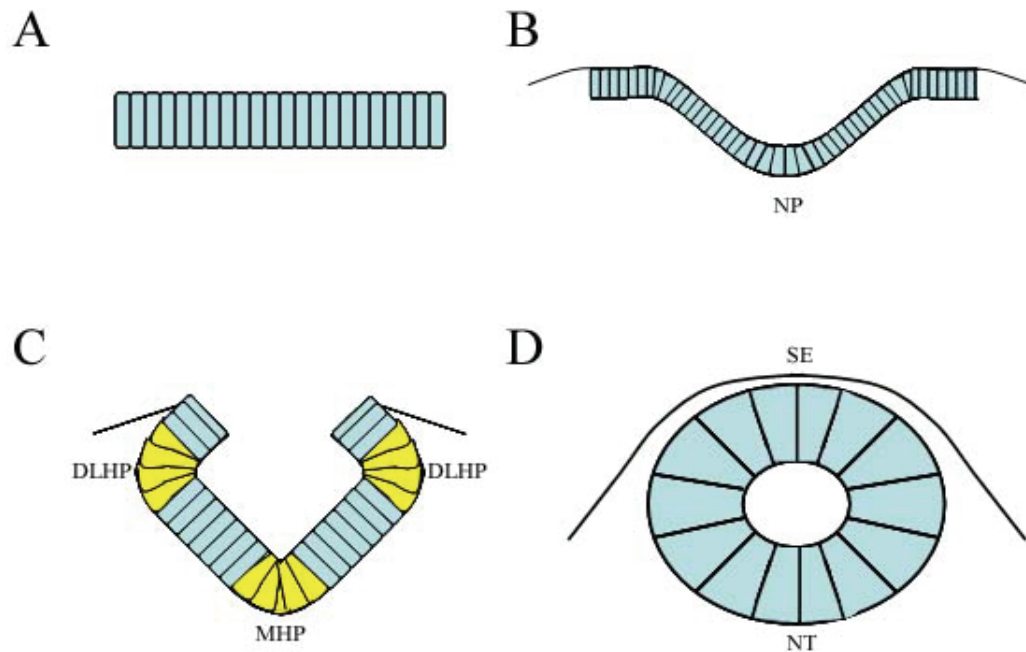


**Figure 3: Morphogenetic movements during neural tube closure**

During neurulation, the neural plate must transform from a flat sheet (A) to a closed tube (D). (B) The process of neural tube closure begins with the elevation of the neural plate (NP). Apical constriction of cells within the medial (MHP) and dorsal lateral hinge points (DLHP) drives the bending and rotation of the neural folds (C). In the final steps of neural tube closure the neural folds meet at the midline and fuse, and the neural tube (NT) separates from the surface ectoderm (SE) (D).

Formation of the hinge points requires cells to undergo dramatic cytoskeletal and cell shape changes, transforming from a columnar shape to a wedge-shape. This change in cellular morphology is believed to occur primarily through the process of apical constriction. During the process of apical constriction, a dense apical actin-myosin belt contracts, resulting in a reduction of the apical surface area relative to the basal surface area (Fig. 4). Because cells of an epithelial sheet are connected to one another by numerous cell adhesions, this reduction in apical surface

area relative to basal surface area would create a pulling force that could drive bending of the neural epithelium.

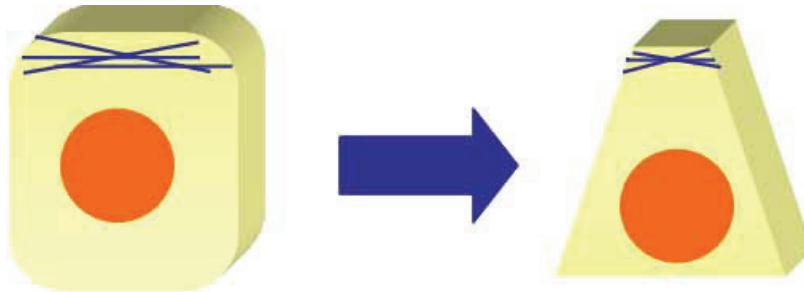


**Figure 4: The purse-string model of apical constriction**

According to the purse-string model of apical constriction, contraction of the apical actin-myosin band causes the apical surface of the cell to shrink, transforming the cell from a columnar shape to a wedge-shape.

Bending of epithelial sheets is required for the morphogenesis of multiple structures in numerous organisms including ventral furrow formation in *Drosophila*, *C. elegans* gastrulation, and optic vesicle formation in vertebrates [47-51]. Apical constriction is known to provide at least some of the mechanical force required for epithelial sheet bending during many of these processes. However, very little is known about the how apical constriction in the vertebrate neural epithelium is regulated on the cellular or molecular level.

Additionally, a slowing of the rate of cell division in the hinge points has been suggested to play a role in cell shape change. In a process known as interkinetic nuclear migration, the nuclei of dividing cells travel between the basal and apical poles [42, 44, 52]. A slowing of the cell cycle in hinge point cells requires the nuclei to remain basal, thus contributing to the basal expansion that accompanies apical constriction [33, 42]. Extrinsic forces involved in neural tube closure include pushing forces generated by the directed mitosis, cell flattening, and intercalation of non-neural ectoderm [33, 42, 49, 53].

Once the neural folds converge at the midline, they undergo fusion. Research in mice has identified three distinct closure points [54]. The first point of closure occurs at the hindbrain/cervical boundary, at approximately embryonic day (e) 8.5 in the mouse. From this first fusion point, neural tube closure proceeds both rostrally and caudally, in a zipper-like fashion. A second closure takes place at the forebrain/midbrain boundary, and closure continues bidirectionally. A final *de novo* closure takes place at the rostral extremity of the forebrain.

## 1.5 THE ROLE OF SHROOM IN NEURAL TUBE CLOSURE

Shrm is required for apical constriction during neural tube closure in mice and *Xenopus* [23, 24]. Homozygous *Shrm* mutant mice exhibit a variety of neural tube defects, including exencephaly, acrania, facial clefting, and spina bifida. Inactivation of Shrm in *Xenopus* embryos by morpholino knockdown or by expression of a dominant-negative form of Shrm inhibits apical constriction and leads to a failure of cranial neural tube closure [23]. Shrm localizes to the stress fibers of fibroblast cell lines and to the apical region of adherens junctions in polarized epithelial lines [24]. Within the neural epithelium of e9.25 mouse embryos, Shrm is restricted to the apical junctional complex. This localization is consistent with the hypothesis that Shrm directs neural tube closure by inducing constriction of the apical actin belt of neural epithelium.

Since its initial characterization, research has revealed that Shrm can induce naïve *Xenopus* epithelium as well as confluent monolayers of MDCK cells to accumulate apical actin and to constrict their apical surface [23]. Failure of apical constriction in Shrm mutants leads to defects in hinge point formation and epithelial sheet bending, resulting in the observed NTDs.

Recent work has shown that Shrm's ability to induce apical constriction and elicit changes in cell shape require the activity of non-muscle myosin II [39].

## **1.6 THESIS OVERVIEW**

Actin binding proteins are involved in a diverse collection of cell processes and behaviors, including migration, cell adhesion, morphogenesis, and vesicular trafficking. The goal of my research has been to investigate the cellular function of a novel actin-binding protein, Apxl. In this thesis, I describe the work I have done in order to provide an initial characterization of Apxl. I have explored the expression pattern of Apxl in adult and embryonic mouse tissues as well as the subcellular localization of Apxl. Analysis of a series of Apxl truncations has helped to elucidate the contribution of each of the three conserved domains to Shrm protein family function. Additionally I have determined that Apxl is capable of binding F-actin through its ASD1 domain. Although no known function exists for Apxl, its expression pattern and its relationship to Shrm suggest that it may play a role in regulation of cellular architecture throughout development.

## **2.0 MATERIALS AND METHODS**

### **2.1 CELL CULTURE**

Rat1 fibroblast and CtBP90 cell lines were maintained in Dulbecco's Modified Eagle Medium (DMEM) with 10% fetal bovine serum (FBS), penicillin/streptomycin, and L-glutamine. MDCK cells were maintained in Eagle's Minimum Essential Media (EMEM) supplemented with 10% FBS, penicillin/streptomycin, and L-glutamine. All cell lines were cultured at 37 ° C and 5% CO<sub>2</sub>. For expression of exogenous Apxl, cells were transfected using 1-2 µg of DNA and Lipofectamine 2000 transfection reagent (Invitrogen) according to the manufacturer's recommendations.

### **2.2 MOLECULAR BIOLOGY**

To create the series of Apxl deletion constructs, portions of Apxl cDNA encoding amino acids 1-513, 1-880, 513-880, 880-1479, and 1-1479 (full-length Apxl) were cloned into the pCS3mt expression vector in frame with the 6X Myc tag. Cloning of Apxl deletion constructs was performed by Teresa Bernaciak and Jennifer Phillips.

### 2.3 ANTIBODIES, WESTERN BLOTTING AND IMMUNOFLUORESCENCE

Apxl-specific sera was generated by Cocalico Biologicals by injecting rabbits with Glutathione S-transferase-tagged Apxl 878-1287 (GST-Apxl 878-1287). Apxl-specific antibodies were affinity purified using GST-Apxl 878-1287 coupled to Sepharose.

For western blotting, cells were lysed on ice in 0.4 mL RIPA buffer (150mM NaCl, 1.0% NP-40, 0.5% sodium deoxycholate, 0.1% SDS, and 50mM Tris pH8.0) with 1mM phenylmethylsulfonyl fluoride (PMSF) and Aprotinin, centrifuged at 13,000 x g, and mixed with an equal volume of 2X Laemmli sample buffer. Embryo and tissue lysates were generated by homogenizing samples in RIPA buffer plus protease inhibitors at 4<sup>o</sup> C with a tissue tearor and mixed with Laemmli sample buffer. All lysates were heated to 100<sup>o</sup> C for five minutes prior to separation by SDS-PAGE and total proteins were transferred to nitrocellulose membranes. Blots were blocked in 4% dehydrated non-fat milk in Tris-Buffered Saline Tween 20 (TBST) for 1 hour at room temperature. Apxl was detected by incubating blots with anti-Apxl (1:100 dilution in 4% milk/TBST) or mouse monoclonal antibody (mAb) 9E10 (anti-myc, 1:200 dilution in 4% milk/TBST) at 4<sup>o</sup> C overnight. Blots were washed 3 times for 5 minutes in TBST prior to addition of secondary antibody. Primary antibodies were detected by incubation with goat anti-rabbit or goat anti-mouse horseradish peroxidase-conjugated secondary antibody (1:2500 in TBST, Amersham) for 1 hour at room temperature, followed by 3 5 minute washes in TBST. HRP-conjugated secondary antibodies were visualized using enhanced chemiluminescence reagents (Amersham).

Prior to immunofluorescent staining, cells were grown on glass coverslips and then fixed in -20<sup>o</sup> C methanol for 5 minutes or 4% paraformaldehyde in phosphate buffered saline (PBS)

for 15 minutes and washed with PBS. Indirect immunofluorescence was performed with affinity-purified anti-ApxI (1:50), rat anti-CD31/PECAM-1 (BD Pharmingen, 1:400), anti-Neurofilament, Rat anti-ZO-1 (1:200, Chemicon), anti-E-cadherin (1:400, BD Pharmingen), mAb anti- $\beta$ -catenin (1:200, BD Pharmingen), and anti-Myc mAb 9E10. All primary antibodies used for immunofluorescence were diluted in PBS/0.1% Tween 20 (PBT). Primary antibodies were visualized using Alexa-488 and -568 conjugated secondary antibodies (1:400, Molecular probes). F-actin was detected with Tetramethylrhodamine B isothiocyanate (TRITC) or Alexa-633 conjugated phalloidin (Sigma and Molecular Probes, respectively).

To generate frozen sections used for immunocytochemistry, embryos or adult tissues were isolated and incubated in 4% paraformaldehyde at 4<sup>o</sup> C for 1-3 hours. Embryos or tissues were then washed in cold PBS, and incubated in 30% sucrose overnight at 4<sup>o</sup> C. Samples were embedded in OCT and 10-12  $\mu$ M sections were cut at -20<sup>o</sup> C using a Leica cryostat. Prior to staining, sections were rehydrated in PBS for 5 minutes at room temperature and blocked in 1% goat serum in PBT for 30 minutes at room temperature. Sections were incubated with primary antibody in 1% goat serum/PBT at room temperature for 2-3 hours or overnight at 4<sup>o</sup> C and washed 3 times in PBT at room temperature. Sections were incubated in secondary antibody diluted in 1% goat serum/PBT for 1-2 hours in the dark at room temperature, then washed in PBT. Slides were mounted using Vectashield mounting medium (Vector Labs). Images were collected using a Biorad Radiance 2000 Laser Scanning System and a Nikon E800 microscope and processed using Adobe Photoshop.

## 2.4 CO-IMMUNOPRECIPITATION

To perform co-immunoprecipitation experiments, whole embryo lysates were generated by homogenizing e10.5 mouse embryos in RIPA buffer plus protease inhibitors with a Dounce homogenizer at 4<sup>o</sup> C. Apx1 was precipitated from 1 mL of whole embryo lysates by incubation with 50 µl anti-Apx1 and 50 µl protein A sepharose beads (Amersham) for 1 hour at 4<sup>o</sup> C with constant rocking. Immune complexes were washed in RIPA buffer to remove unbound proteins and resuspended in Laemmli sample buffer. Beads were heated to 100<sup>o</sup> C to uncouple immunoprecipitated proteins from the beads, and proteins were separated by SDS-PAGE and transferred to nitrocellulose membranes. Blots were probed with anti-Apx1 (1:250), Rat anti-ZO-1 (1:400, Chemicon), anti-Occludin (1:200, Santa Cruz), mAb anti-β-catenin (1:400, BD Pharmingen), and anti-Vinculin (1:200, Sigma) diluted in TBST+ 4% milk.

## 2.5 ACTIN BINDING

In order to perform the actin cosedimentation experiment, a GST-Apx1513-880 fusion protein was expressed in BL21 *E. Coli* and purified using glutathione-sepharose. F-actin was prepared by polymerization of G-actin (Cytoskeleton). For cosedimentation assays, GST-Apx1513-880 was incubated for 1 hour at room temperature in the presence or absence of 0.08 µM polymerized F-actin. F-actin was pelleted by centrifugation at 100,000 x g in an airfuge and pellet and supernatant fractions were collected. Proteins were separated by SDS-PAGE and visualized with Coomassie blue.

### **3.0 EXPRESSION PROFILE OF APXL**

#### **3.1 RESULTS**

Initial characterization of Apxl began with a survey of its expression pattern in mice. In order to determine when and where Apxl is expressed, a polyclonal antibody to amino acids 878 to 1287 was generated and used for Western blot analysis and indirect immunofluorescence. Anti-Apxl antibodies, but not pre-immune antibodies, detect a protein of approximately 210 kDa in both whole embryo lysates and immunoprecipitations from e10.5 mice. Although the predicted molecular mass for *Apxl* is 165 kDa, a molecular mass of 210 kDa is consistent with the observed molecular mass of other Shrm family members [24, 55]. Protein lysates were made from a variety of adult tissues, and Western blots were probed with Anti-Apxl (Fig. 5). Apxl was detected in the majority of tissues tested, including the brain, lung, stomach and heart. To further characterize Apxl in adult and embryonic mice, indirect immunofluorescence was performed on frozen sections using the Anti-Apxl antibody.

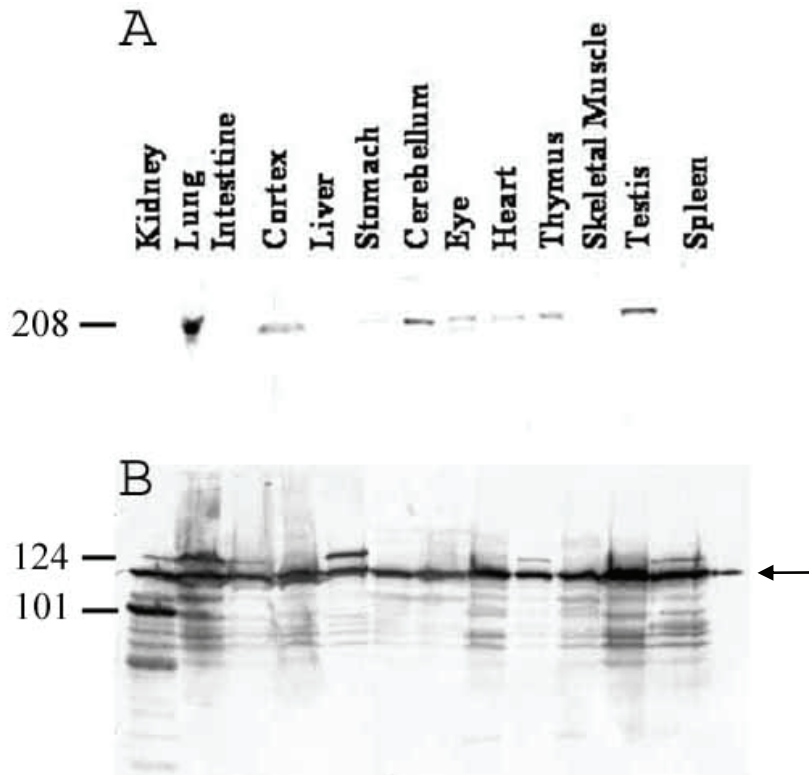


**Figure 5: Apxl is widely expressed in adult tissue lysates**

Lysates of numerous adult mouse tissues were analyzed by immunoblotting (A). An approximately 210 kDa band corresponding to Apxl was detected in lung, brain, eye, heart, thymus, and testis lysates. (B) Blots were probed with an anti-Vinculin antibody as a loading control. The approximately 116 kDa Vinculin band was observed in all lanes (arrow).

Mouse embryos of various ages were cyrosectioned and stained to detect Apxl. In e10.5 embryos Apxl expression can be detected in the cranial neural tube (Fig. 6A and 6B). Like Shrm, Apxl colocalizes with cortical actin in the apical portion of neuroepithelial cells (Fig. 6B). Detectable levels of Apxl expression were consistently observed in structures that resembled the embryonic vasculature. In order to verify this, sections were stained to detect Apxl and platelet endothelial cell adhesion molecule-1 (PECAM-1). PECAM-1 is a member of the immunoglobulin family of cell adhesion molecules. Because PECAM-1 is expressed in the vascular system in both developing and adult organisms, it is commonly used as an endothelial

cell marker [56-59]. Figure 6A shows Apxl colocalizing with PECAM-1 in blood vessels. In addition to its function as an adhesion molecule, PECAM-1 has also been identified as a scaffold for signaling and adaptor proteins [56-59]. Similar co-localization of Apxl and PECAM-1 in embryonic vasculature was observed throughout the embryo. Expression of Apxl within the vasculature likely explains the broad distribution of Apxl positive tissue lysates detected by Western blot.

Apxl is also expressed in the dorsal root ganglia (Fig. 6). Figures 6C and 6D show that at e10.5 and e12.5, respectively, Apxl expression is limited to the PECAM-positive vasculature surrounding the dorsal root ganglia. By e15, however, cells of the dorsal root ganglia expressing the neuron marker Neurofilament (NF) have begun to express Apxl.

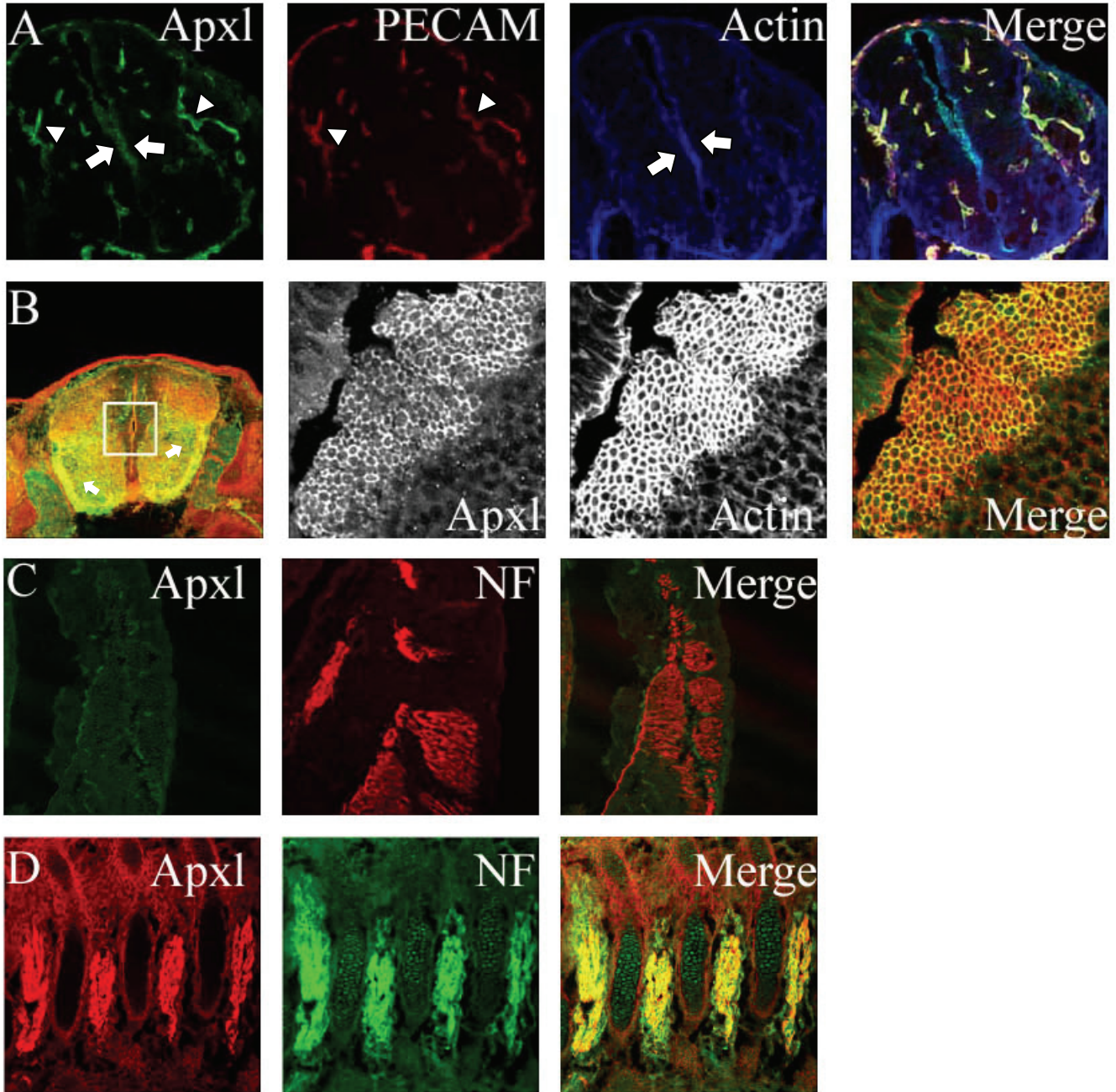


**Figure 6: Apxl localizes to the apical surface of neural epithelium and to dorsal root ganglia**

(A) Sections through an e10.5 neural tube were stained for Apxl (green), PECAM (red), and F-Actin (phalloidin, blue). Apxl colocalizes with actin at the apical surface of the neural epithelium (arrows), as well as with PECAM in the vasculature of the neural tube (arrowheads). (B) A magnified view of Apxl and Actin staining within the neuroepithelium of an e16.5 mouse. Apxl also appears to localize to differentiated neurons at this stage (arrows in B). At e15 Apxl is express in NF-positive cells of the dorsal root ganglia (D), but not at e10.5.

Although Apx1 expression was not detected in Western blots of adult kidney and intestinal lysates, specific expression was detected by immunostaining of these tissues (Fig. 7, 8). Apx1 expression was detected within the apical membrane of renal and intestinal epithelial cells. Frozen adult kidneys were sectioned and stained for Apx1, ZO-1 and Actin. Specific expression was detected in the apical membrane of a subset of renal tubules, which may explain the inability to detect a strong Apx1 band in Western blots (Fig. 7). Within the collecting ducts Apx1 colocalized with actin and displayed partial overlap with ZO-1. No co-localization was observed between Apx1 and the adherens junction protein,  $\beta$ -catenin (Fig. 7B).

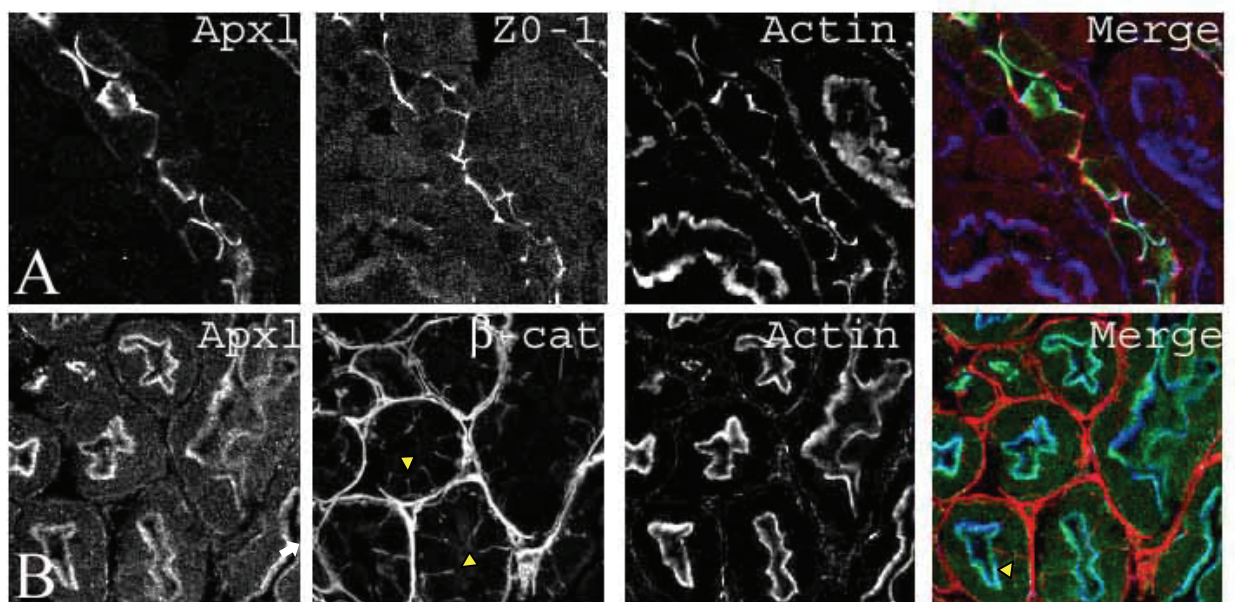


**Figure 7: Apx1 is expressed in renal collecting ducts**

Sections of adult kidney stained for Apx1 show localization to the apical surface of the renal collecting duct (A, B). Within renal tubules Apx1 colocalizes with ZO-1 and actin (A), but not  $\beta$ -catenin, (yellow arrowheads in B).

Apxl also localized to the apical surface of intestinal epithelial cells. Frozen sections of adult intestine were sectioned and stained for Apxl,  $\beta$ -catenin, and PECAM. Figures 8A and 8B show Apxl localizing to the apical membrane of intestinal cells and not to the  $\beta$ -catenin positive lateral membranes. Although Apxl localizes to the embryonic vasculature, no co-localization is detected between Apxl and the endothelial cell marker, PECAM, in adult intestine.

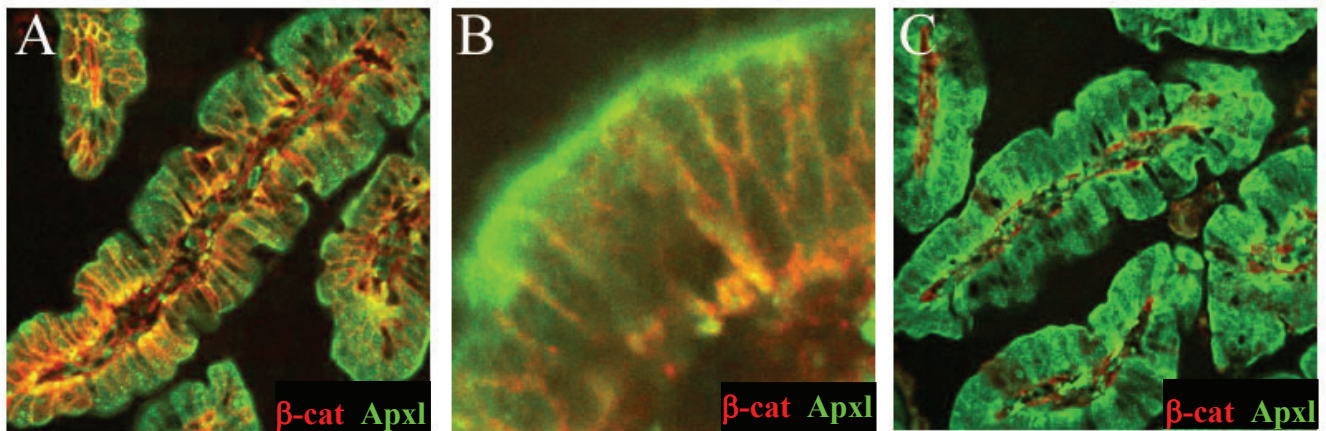


**Figure 8: Apxl is expressed in adult intestine**

(A, B) Apxl localizes to the apical membrane in cells of the adult mouse intestine (Apxl in green,  $\beta$ -catenin in red). (C) Apxl is not expressed in the vasculature of the adult intestine, as shown by a lack of colocalization with PECAM (red)

### 3.2 DISCUSSION

Western blot and immunofluorescence analysis reveal that Apxl is expressed in numerous tissues throughout the developing mouse, including the neural epithelium, vasculature, kidney, and

intestine. Apxl seems to be specifically expressed in polarized epithelial or endothelial cell types, where it resides at or near the apical membrane and junctional complexes.

Regions of Apxl expression show a high degree of overlap with Shrm's expression pattern, suggesting the possibility that Shrm and Apxl may function in some of the same morphogenetic and cellular processes. Within the neural epithelium, Shrm and Apxl both colocalize with ZO-1 and actin at the apical border of the lateral membrane. Shrm and Apxl also localize similarly in renal tubules.

Apxl expression in the kidney is particularly interesting in light of Apxl's relation to Apx. Apx forms a complex with the renal epithelial sodium channel, ENaC, and  $\alpha$ -spectrin. ENaC constitutes the main mechanism for  $\text{Na}^+$  absorption in the connecting tubule as well as other aldosterone-responsive transporting epithelia such as the colon and fetal lung [29, 60]. Sucrose density gradient centrifugation and immunoblot analysis from *Xenopus* A6 cells indicate that in ENaC, Apx, and  $\alpha$ -spectrin are associated in a macromolecular complex, suggesting that Apx is required for the functional expression of ENaC in *Xenopus* epithelia [28]. In support of this hypothesis, *Xenopus* oocytes coinjected with ENaC cRNA and Apx antisense oligonucleotides showed a marked reduction in amiloride-sensitive current compared to oocytes coinjected with Apx sense oligonucleotides [28]. However, although Apx is believed to regulate ENaC conductance in *Xenopus* kidneys, the relationship between Apxl and ENaC, if any, remains undetermined.

Transport across epithelial and endothelial barriers occurs through transcellular or paracellular pathways. Within the kidney, renal absorption and paracellular permeability are controlled, in part, by alterations in tight junction permeability. Paracellular transport through absorptive epithelia, such as the kidney and small intestine, is mediated largely by tight junction

composition. Claudin proteins exhibit distinct tissue expression patterns and this differential expression helps to regulate the permeability of tight junctions [17, 61, 62]. Studies of paracellular permeability frequently utilize Madin-Darby Canine Kidney (MDCK) cells as a model of barrier epithelia. Type I MDCK cells resemble cells of the distal collecting ducts and exhibit high electrical resistance, whereas type II MDCK cells are considered to be representative of the proximal tubule and display low electrical resistance [63-65]. Expression of claudin-2 in type I MDCK cells that normally express claudin-1 and -4 decreased transepithelial electrical resistance (TER) and increased paracellular permeability [17]. Conversely, over-expression of claudin-1 in MDCK cells dramatically increased TER and reduced paracellular permeability [66].

Apxl localizes to the apical membrane of renal tubules, where it shows some degree of overlap with the tight junction marker ZO-1. Additionally, Apxl localizes to the apical surface of intestinal epithelia. Furthermore, Apxl is highly expressed in the vascular endothelium, another structure where paracellular permeability is tightly regulated. This expression pattern and subcellular localization suggests the possibility that Apxl is involved in regulation of paracellular transport in the mammalian kidney and intestine. Attempts to observe the co-localization of Apxl with various claudins were inconclusive due to a lack of good antibodies. Much work remains to be done to elucidate the role, if any, Apxl plays in Na<sup>+</sup> absorption or paracellular permeability.

## **4.0 APXL LOCALIZES TO SITES OF CELL ADHESION**

### **4.1 RESULTS**

#### **4.1.1 Immunoprecipitation and Immunofluorescence**

Initial surveys of Apxl expression in embryonic mice suggested that like Shrm, Apxl was expressed primarily in polarized epithelial cells. More specifically, Apxl frequently localized to the cell membrane. Primary mouse cells were cultured and stained for endogenous Apxl in order to explore the subcellular localization of Apxl. Results from these initial experiments show that within these cells Apxl resides at the plasma membrane where it colocalizes with AJ proteins such as  $\beta$ -catenin and with the TJ marker, ZO-1 (Fig. 9). While Apxl costains with the adherens junction protein E-cadherin, Apxl displays a much more specific co-localization with ZO-1 in polarized cells.

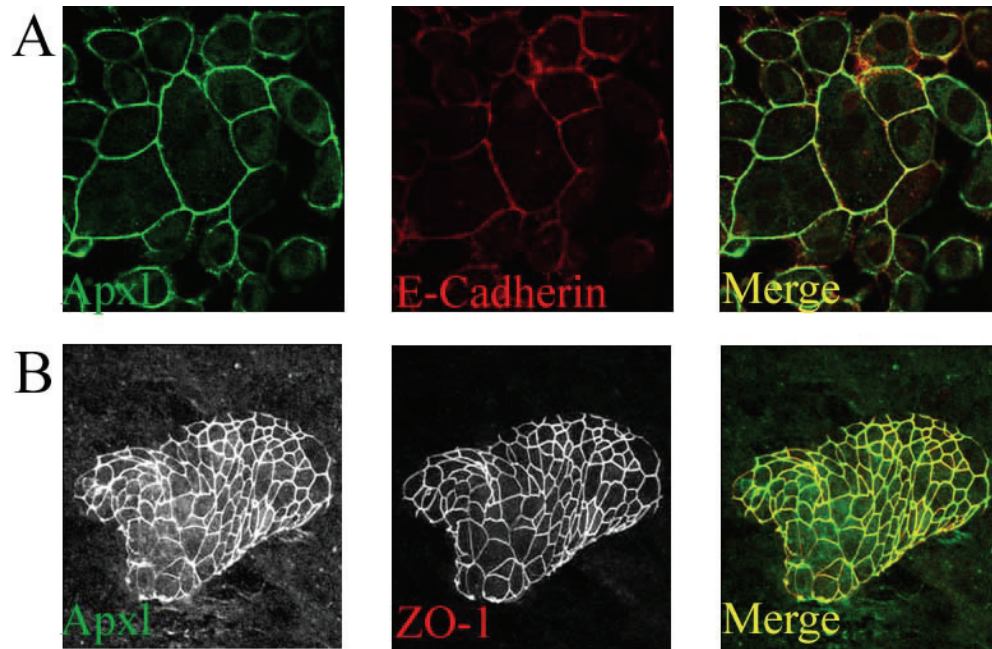


**Figure 9: Apxl localizes to cell adhesions**

Primary mouse embryos were cultured and stained for Apxl, ZO-1, and E-Cadherin. Apxl localizes to sites of cell adhesion with both E-Cadherin (A) and ZO-1 (B).

To further investigate the localization of Apxl in a polarized epithelial cell line, MDCK cells were utilized as a model cell line. MDCK cells transiently transfected with an epitope-tagged version of the protein were grown on glass coverslips and stained for Apxl and ZO-1 (Fig. 10). Although a large portion of Apxl remained cytoplasmic, a significant population of Apxl was observed at ZO-1-positive TJs (Fig. 10B, arrow). Apxl was not observed in the lateral membranes of transfected cells, suggesting that Apxl is specifically recruited to TJs or to other components of the apical junctional complex.

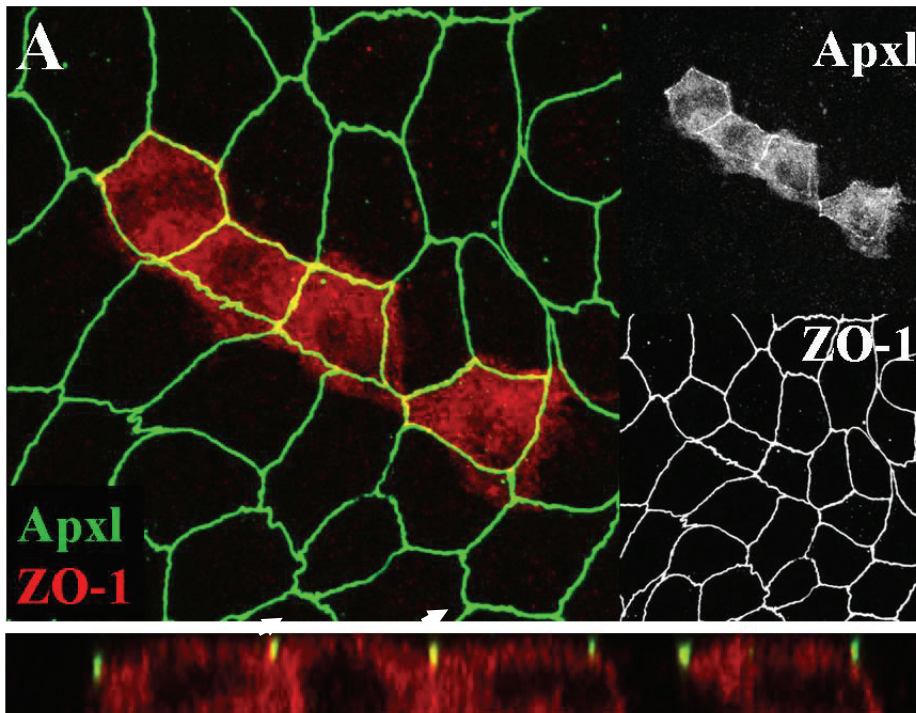


**Figure 10: Apxl localizes to tight junctions in MDCK cells**

Within a monolayer of MDCK cells, a portion of Apxl localizes to ZO-1-positive tight junctions (A and arrows in B). Only partial co-localization is observed, as a significant portion of Apxl remains cytoplasmic (A).

To determine how Apxl is recruited to sites of cell-cell adhesion, a series of co-immunoprecipitation (Co-IP) experiments were performed. Because Apxl is frequently observed colocalizing with junctional proteins such as  $\beta$ -catenin and ZO-1, I hypothesized that Apxl might be in a complex with one or more junctional proteins. Apxl was immunoprecipitated from whole embryo lysates using the Apxl antibody. Co-IPs were analyzed by Western blot and blots were probed with antibodies to several cell adhesion proteins (Fig 11). Apxl was successfully immunoprecipitated from embryo lysates (Fig. 11E). Despite the presence of Apxl at tight junctions no interaction was detected between Apxl and the TJ proteins ZO-1 or Occludin (Fig 10 B, D). Additionally, no interaction was detected between Apxl and  $\beta$ -catenin or the focal

adhesion/adherens junction protein, Vinculin (Fig. 11 A, C). These results suggest that Apxl does not directly bind to these junctional proteins. Alternatively, large protein complexes may have been disrupted by the co-immunoprecipitation protocol.

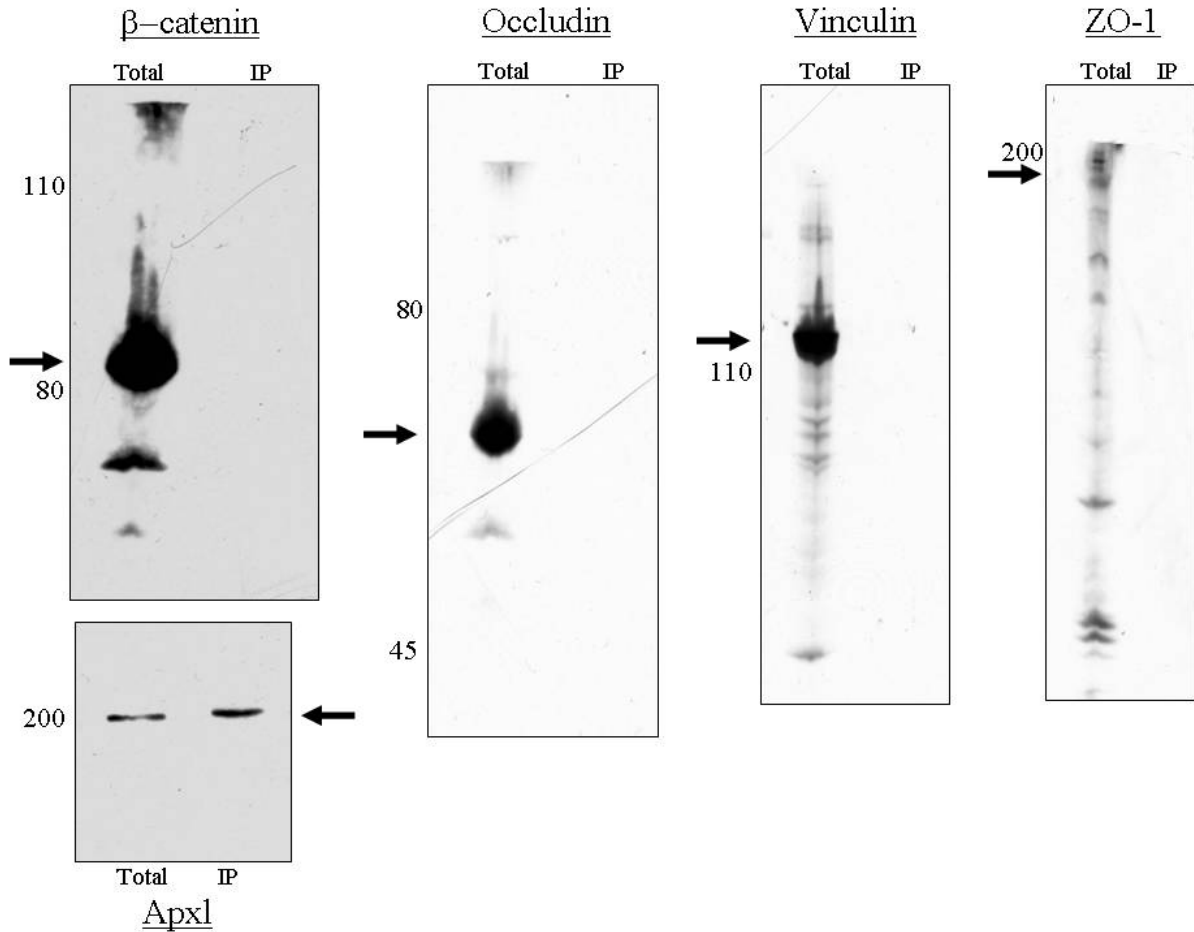


**Figure 11: Apxl co-immunoprecipitation experiments**

Apxl was immunoprecipitated from whole embryo lysates and blots were probed with  $\beta$ -catenin (A), Occludin (B), Vinculin (C), and ZO-1 (D). None of the candidate adhesion proteins tested co-immunoprecipitated with Apxl, although Apxl was visible in control blots (E). Arrows indicate  $\beta$ -catenin, Occludin, Vinculin, ZO-1, and Apxl bands, respectively.

#### 4.1.2 Apxl Deletion Constructs

To investigate the contribution of each protein domain to the localization of Apxl, a series of Apxl deletion constructs were generated and expressed in three mammalian cell lines (Fig. 12). With the assistance of Teresa Bernaciak, Apxl cDNA was cloned into the CS3mt vector, adding a 6X myc tag to facilitate detection of the exogenous proteins. These deletion constructs were initially expressed in CtBP90 cells, a fibroblast cell line which displays some epithelial characteristics due to mutations in *ctbp1* and *ctbp2* [67]. CtBP90 cells express endogenous Apxl, allowing comparison of endogenous and transfected Apxl by staining with anti-Apxl or anti-myc antibodies, respectively. When these deletion constructs were expressed in CtBP90 cells, proteins of the appropriate molecular weight were detectable by Western blot (Fig 12 B). All Apxl deletion proteins, with the exception of Apxl 1-513, were detected by both the anti-Apxl and anti-myc antibodies. Because the Apxl antibody was generated to amino acids 878-1287, Apxl 1-513 could only be detected by staining for the myc tag.

In order to investigate their ability to interact with actin, the full complement of Apxl constructs was expressed in Rat1 fibroblasts, which display an extensive actin cytoskeleton. Finally, Apxl deletion constructs were also expressed in MDCK cells in order to explore their localization to the apical junctional complex. Full-length Apxl co-localized with endogenous Apxl at the membranes of CtBP90 and Rat1 fibroblasts (Fig 13A). In the MDCK cell line, Apxl co-localized with ZO-1 at tight junctions. Additionally, Apxl staining of CtBP90 cells revealed localization to several focal adhesion-like structures.

A construct possessing only the first 513 amino acids of Apxl does not localize similarly to full-length Apxl. Apxl 1-513 localized weakly to tight junctions in MDCKs and was found in

the cytoplasm of Rat1 and CtBP90 cells (Fig 13B). Despite the inclusion of the PDZ domain, this N-terminal portion of Apxl does not act as the localization domain in these cell lines.

Apxl 1-880, containing both the PDZ and ASD1 domains, displayed very strong membrane localization in the fibroblast cell lines, similar to the localization displayed by the full-length construct as well as endogenous Apxl (Fig. 13C). Apxl 1-880 also exhibited tight junction localization in the MDCK cell line.

Apxl 513-880, containing only the ASD1, domain failed to localize at the membrane in CtBP90 and MDCK cells (Fig. 13D). Apxl 513-880 was detected in the cytoplasm in CtBP90 and MDCK cells, although it localized to the membrane of Rat1 cells. Similarly, Apxl 513-1479, which possesses both the ASD1 and ASD2 domains, localized to the membrane of CtBP90 and Rat1 cells, while remaining cytoplasmic in the MDCK cell line (Fig. 13E). Finally, a C-terminal expression construct containing only the ASD2 domain, Apxl 880-1479, failed to localize to the membrane or junctional complexes in all three cell lines tested (Fig. 13F). Figure 16 summarizes the sub-cellular localization of all Apxl deletion constructs in the cell lines tested.

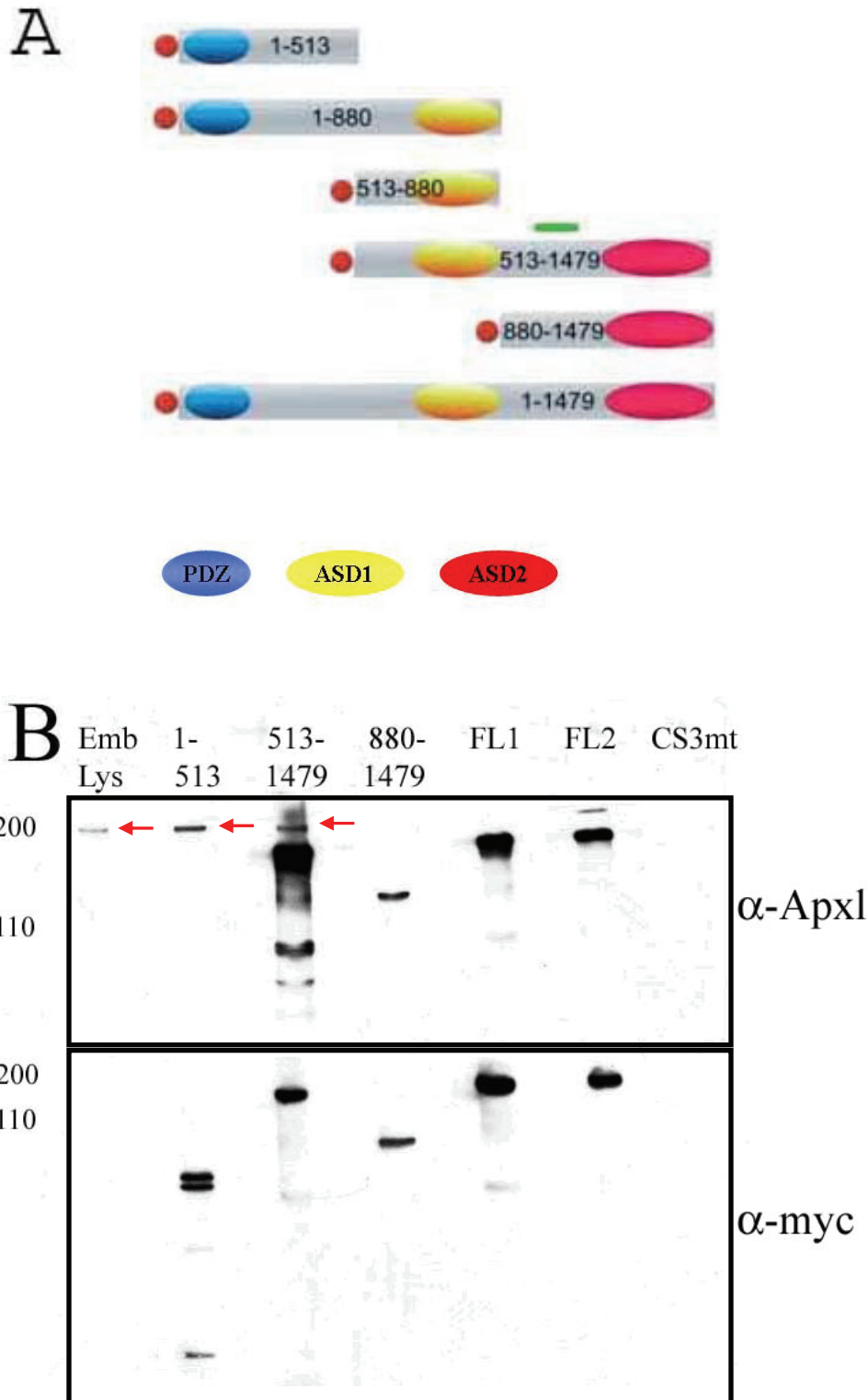


**Figure 12: Apxl deletion constructs**

(A) A series of Apxl deletion constructs were generated in order to explore the contribution of each protein domain to Apxl localization. Apxl 1-513 was not detectable with the Apxl antibody, but endogenous Apxl was detected (red arrows in A) Green bar represents region used to generate Apxl antibody. (B) Deletion constructs were expressed in

CtBP90 cells and analyzed by Western blotting. Proteins of the correct size were detected on blots probed with antibodies which recognized Apx1 (top panel) or the 6X –myc tag (bottom panel) FL1, F12 are full-length version of Apx1. CS3mt represents the empty myc-tagged vector.

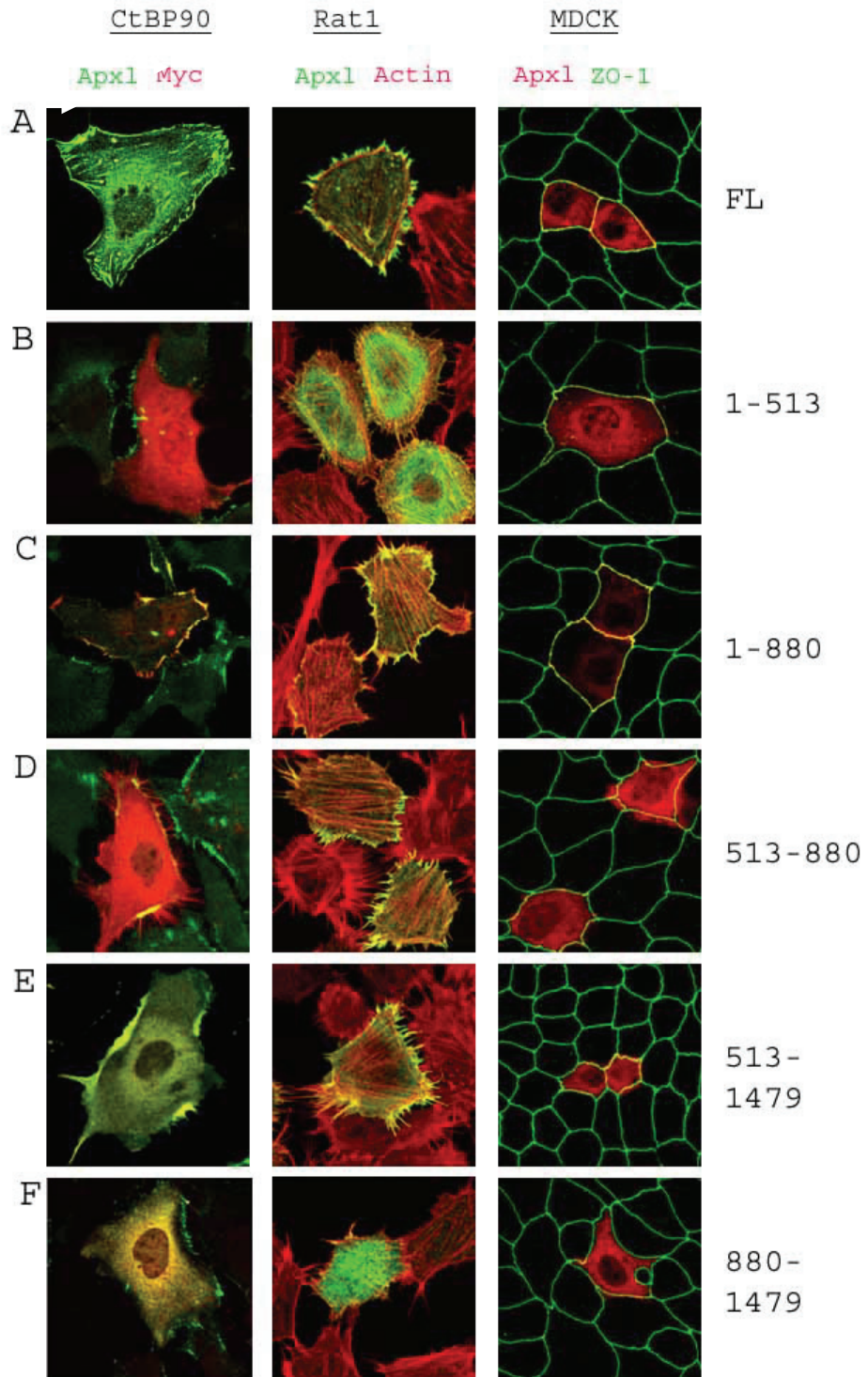


**Figure 13: Localization of Apxl truncation proteins varies with cell type**

Full-length (A) and truncated Apxl proteins (B-F) were expressed in CtBP90, Rat1, and MDCK cell lines and the subcellular localization of Apxl was observed. CtBP90 cells were stained with antibodies to Apxl (green) and the myc epitope tag (red) in order to compare transfected and endogenous Apxl protein. Rat1 fibroblasts expressing Apxl deletion constructs were stained to detect Apxl (green) and actin (red). MDCK cells were stained with Apxl (red) and the tight junction marker ZO-1 (green) to view Apxl targeting to tight junctions.

**4.1.3 Apxl binds actin but does not cause apical constriction**

Because Apxl consistently localizes with the actin population in multiple cell types, we examined whether the actin cytoskeleton positions Apxl. When cells are treated with Cytochalasin D the actin cytoskeleton collapses. Additionally, actin-binding proteins which depend on actin for proper localization become mislocalized, while other proteins such as Vimentin and the neural recognition molecule L1 retain normal localization [68, 69]. Mouse cells (CtBP90) were treated with Cytochalasin D to block actin polymerization, resulting in a collapse of the actin cytoskeleton. After 20 minutes, the distribution of Apxl collapsed along with the actin cytoskeleton (Fig. 14). This dependence on the actin cytoskeleton for proper localization suggests that Apxl localization is dependent on F-actin and that Apxl resides in a complex with actin.

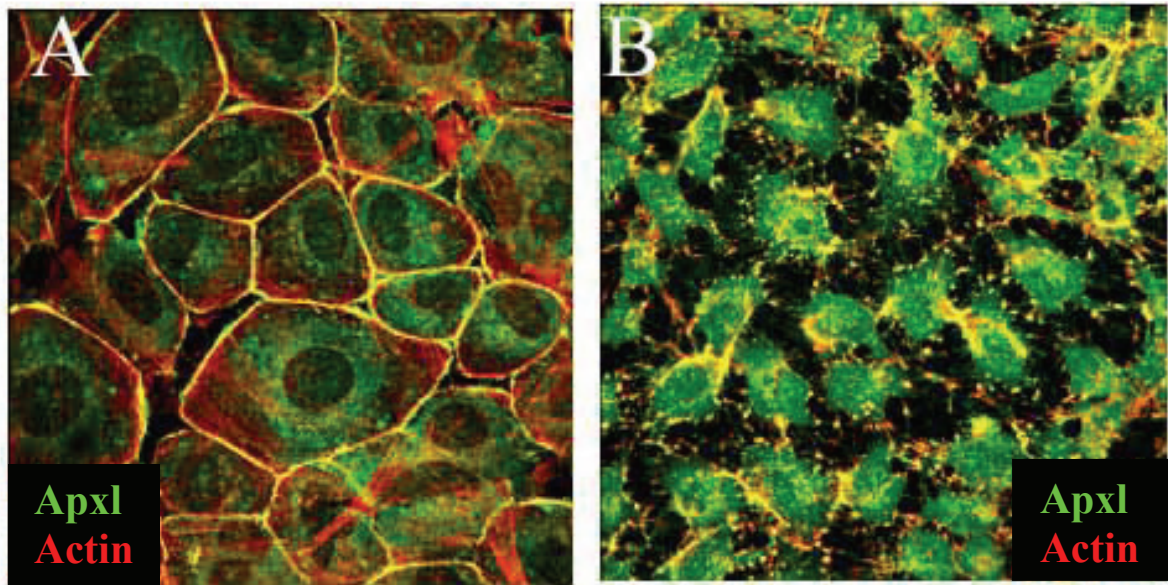


**Figure 14: Apxl localization collapses after cytochalasin treatment**

Cells expressing Apxl were stained to detect Apxl (green) and F-actin (red). In untreated cells Apxl localizes with cortical actin at the cell membrane (A). After cytochalasin treatment to breakdown F-actin, Apxl loses its membrane localization (B) but remains associated with actin, suggesting that Apxl associates with F-actin.

Previous research has determined that the ASD1 domain of Shroom directly binds F-actin filaments, and recent work has shown that the ASD1 of Apxl can bind actin as well [24, 70]. Because Apxl possess a similar ASD1 domain, and Apxl localization is dependent on cytoskeletal integrity, actin co-sedimentation experiments were performed using a GST-tagged portion of Apxl containing the ASD1 domain (amino acids 513-880). GST-Apxl 513-880 was incubated with F-actin for one hour at room temperature. F-actin was pelleted by centrifugation at 100,000 X g. GST-Apxl 513-880 remained in the soluble fraction in the absence of actin [70]. However, when F-actin is added to the assay, GST-Apxl 513-880 co-sediments in the fraction

[70]. The presence of Apxl in the pellet fraction of the co-sedimentation experiment shows that the Apxl ASD1 domain is capable of directly binding F-actin.

Although Apxl and Shrm have highly similar ASD1 domains which are capable of binding F-actin in co-sedimentation experiments, these proteins appear to interact differently with actin *in vivo* (Fig. 15). When Rat1 cells, transfected with Apxl or Shrm, are stained for Shrm and F-actin, Shrm can be seen localizing to actin stress fibers (Fig. 15 A). However, Apxl only binds cortical actin and is not observed on stress fibers (Fig. 15 B).

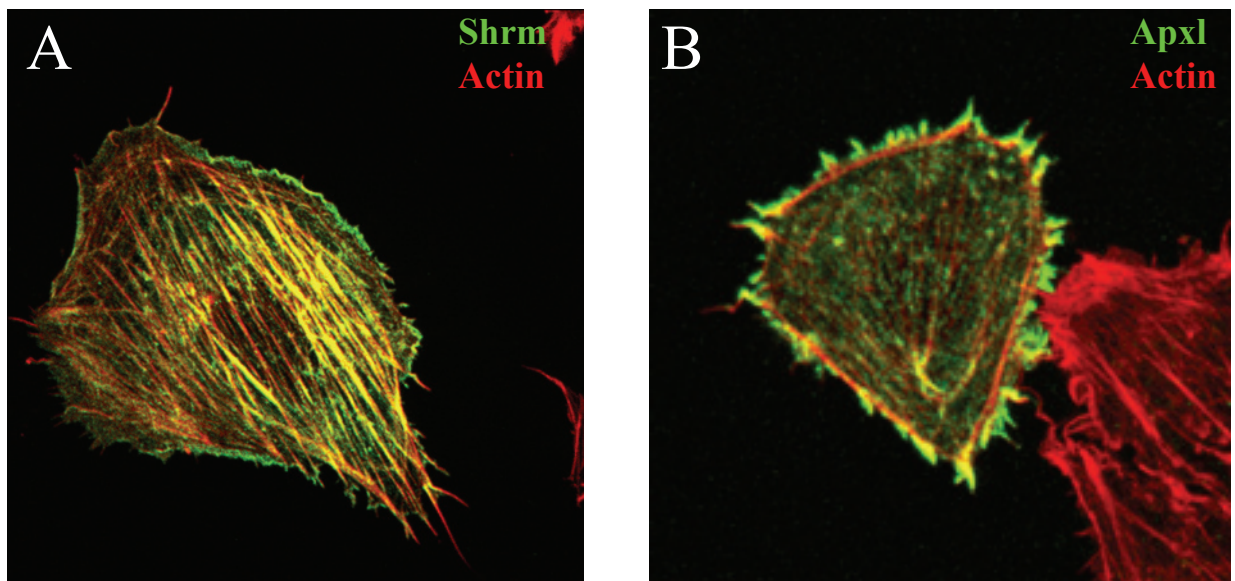


**Figure 15: Apxl localizes to cortical actin but not to stress fibers**

Although the ASD1 domains of Apxl and Shrm bind F-actin in cosedimentation experiments, they appear to interact differently with F-actin *in vivo*. Rat1 cells were transfected and stained for Apxl or Shrm. Shrm prominently stains actin stress fibers in Rat1 fibroblasts (A), while Apxl localization is limited to cortical actin (B).

## 4.2 DISCUSSION

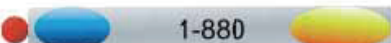
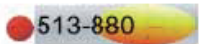
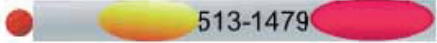
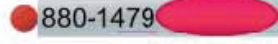
Investigation of the subcellular localization of Apxl reveals that Apxl resides at the plasma membrane of sub-confluent cells and in the plasma membrane of polarized cells, possibly through interactions with cortical actin or members of the apical junctional complex. The high degree of co-localization between Apxl and ZO-1 at the apical/lateral border suggests Apxl is recruited to tight junctions. However, Apxl recruitment to TJs is not complete in MDCK cells, and significant amounts of Apxl remain in the cytoplasm, possibly due to over-expression of Apxl in these cells (Fig 12). Another possibility is that there is a specific mechanism for recruiting Apxl to TJs which functions differently in MDCK cells. Overall, the subcellular localization of Apxl observed in culture correlates well with the observed expression of Apxl in mouse embryos. Apxl consistently localizes to sites of cell-cell adhesion in neural or renal epithelium, as well as in a polarized endothelial cells (Fig. 6, 7).

Many questions remain as to how Apxl is localized in cells, and binding partners for Apxl remain to be identified. Immunoprecipitation experiments, which could have hinted at the functional importance of Apxl, failed to detect any interaction between Apxl and candidate adhesion proteins.

Analysis of Apxl deletion proteins provided more insight into how Apxl is properly localized in the cell (Fig. 16). Although localization varied based on cell type, within all cell lines tested the ASD1 domain is crucial for proper localization. Both Apxl 1-513 and 880-1479, which lack the ASD1 domain, remain cytoplasmic in most cases. The ASD1 domain of Shrm has been shown to interact with F-actin, suggesting that this requirement for the ASD1 domain for Apxl localization is also due to an interaction with cortical actin. However, Apxl 513-880, which contains the ASD1 domain alone, does not localize to the plasma membrane as well as expected,

and it has not been shown to be sufficient for proper membrane/tight junction localization. Apxl 513-880 only maintained membrane localization in Rat1 cells, suggesting that other protein domains contribute to Apxl localization *in vivo*. Alternatively, it is possible that Apxl 513-880 does not localize to the membrane because this fragment fails to fold correctly in some contexts.

Interestingly, it appeared that Apxl 1-880 displayed more intense membrane/tight junction localization than the full-length protein. This suggests that the ASD2 domain may act as a negative regulator of Apxl localization and, possibly, function. Finally, the contribution of the N-terminal PDZ domain for proper localization remains ambiguous. The PDZ domain appears to be irrelevant for normal Shrm localization and function. Although Apxl 513-1479 localizes to the plasma membrane in fibroblasts, it remains primarily cytoplasmic in MDCK cells. In contrast to Shrm, the Apxl PDZ domain contributes to localization in MDCK cells, either by binding to other proteins at the AJC or by influencing protein stability and conformation.

	<u>CtBP90</u>	<u>Rat1</u>	<u>MDCK</u>
 1-513	Cytoplasm	Cytoplasm	weak Tight Junction
 1-880	Membrane, FA	Membrane	Tight Junction
 513-880	Cytoplasm	Membrane	Cytoplasm
 513-1479	Membrane	Membrane	Cytoplasm
 880-1479	Cytoplasm	Cytoplasm	Cytoplasm
 1-1479	Membrane, FA	Membrane	Tight Junction

**Figure 16: Summary of Apxl localization**

The subcellular localization of FL and truncated Apxl constructs varies in the different cell types tested. Constructs lacking the ASD1 domain do not localize correctly in most cases, suggesting that this region of the protein plays a

crucial role in localization. The failure of Apxl 513-880 to localize to correctly in CtBP90 and MDCK cells suggests that this region ASD1 is required but not sufficient for proper localization.

Although much remains to be determined about how Apxl is correctly localized, it is clear that proper distribution of Apxl depends, at least in part, on the ability of Apxl to bind F-actin through its ASD1 domain. Cytochalasin D treatments have shown that disrupting the actin cytoskeleton perturbs Apxl localization, and actin sedimentation experiments have shown that Apxl binds F-actin directly. However, the observation that Apxl is capable of binding actin raises additional questions as to how Apxl and Shrm differ in the interactions with F-actin. Apxl and Shrm share three conserved domains, yet Shrm prominently decorates stress fibers while Apxl cannot. A possible explanation for the differential localization patterns of Apxl and Shrm is that these proteins bind distinct adaptor proteins that help facilitate interactions with F-actin. Identification of binding partners for both Apxl and Shrm would help to explain how these proteins interact with actin. However, the question of how proteins localize to specific populations of F-actin is a fundamental question asked of many actin-binding proteins.

Furthermore, the Shroom and Apxl differ in their ability of cause apical constriction. Shroom has been shown to cause apical constriction in naïve *Xenopus* epithelial cells as well as in MDCK cells [23, 39]. This constriction of the apical surface is dependent Shrm's ability to interact with cortical actin. Despite sharing Shrm's ability to bind actin, Apxl is not competent to induce apical constrictions in MDCK cells [70]. This could be due to an inherent inability to induce constriction, or to differences in how Shrm and Apxl interact with F-actin. However, recent research utilizing chimeric Shrm proteins has shown that the Apxl ASD2, when placed in the context of Shrm, can induce apical constriction in MDCK cells [30]. Therefore, it is possible that the inability of Apxl to induce apical constriction is related to its mechanism of interaction

with actin. In support of this hypothesis, additional work from the Hildebrand lab has shown a correlation between actin bundling by Shrm chimeras and the ability to induce apical constriction.

## 5.0 SUMMARY AND CONCLUSIONS

Western blot and immunofluorescence analysis reveal that Apxl is expressed in numerous tissues throughout the developing mouse, including the neural epithelium, vasculature, kidney, and intestine. In the adult and embryonic mice, Apxl expression seems to be limited to polarized epithelial and endothelial cells, where it resides at or near the apical membrane and junctional complexes. Regions of Apxl expression show a high degree of overlap with Shrm's expression pattern, suggesting the possibility that Shrm and Apxl may function in some of the same morphogenetic and cellular processes.

At the subcellular level, Apxl resides at the plasma membrane of non-adherent cells and in the apical compartment of polarized cells. Apxl may be recruited to these sites through interactions with cortical actin or members of the apical junctional complex. Overall, the subcellular localization pattern observed in culture correlates well with the observed expression of Apxl in mouse embryos. Cytochalasin D treatments and F-actin cosedimentation experiments (performed by Frank Vendetti) have indicated that Apxl binds F-actin through its ASD1 domain. Although additional binding partners of Apxl have not been identified, Apxl consistently localizes sites of cell adhesion in neural or renal epithelium, as well as in a polarized endothelial cell line.

Analysis of Apxl deletion constructs has shown that the actin-binding ASD1 domain is crucial for proper localization and that the ASD2 domain may act as a negative regulator of Apxl

localization. However, the requirement for the N-terminal PDZ domain for Apxl localization and function remains ambiguous. Although the biological function of Apxl is unknown, its expression pattern, subcellular localization, and similarity to Shroom suggest that Apxl may play a role in regulating cellular architecture throughout development.

## BIBLIOGRAPHY

1. Cox, R.T., C. Kirkpatrick, and M. Peifer, *Armadillo is required for adherens junction assembly, cell polarity, and morphogenesis during Drosophila embryogenesis*. J Cell Biol, 1996. **134**(1): p. 133-48.
2. Pollard, T.D. and G.G. Borisy, *Cellular motility driven by assembly and disassembly of actin filaments*. Cell, 2003. **112**(4): p. 453-65.
3. Revenu, C., et al., *The co-workers of actin filaments: from cell structures to signals*. Nat Rev Mol Cell Biol, 2004. **5**(8): p. 635-46.
4. Ridley, A.J., et al., *Cell migration: integrating signals from front to back*. Science, 2003. **302**(5651): p. 1704-9.
5. dos Remedios, C.G., et al., *Actin binding proteins: regulation of cytoskeletal microfilaments*. Physiol Rev, 2003. **83**(2): p. 433-73.
6. Winder, S.J. and K.R. Ayscough, *Actin-binding proteins*. J Cell Sci, 2005. **118**(Pt 4): p. 651-4.
7. Walker, J.L., A.K. Fournier, and R.K. Assoian, *Regulation of growth factor signaling and cell cycle progression by cell adhesion and adhesion-dependent changes in cellular tension*. Cytokine & Growth Factor Reviews, 2005. **16**(4-5): p. 395-405.
8. Woodward, A.M. and D.H. Crouch, *Cellular distributions of the ERM proteins in MDCK epithelial cells: regulation by growth and cytoskeletal integrity*. Cell Biol Int, 2001. **25**(3): p. 205-13.
9. Lambrechts, A., M. Van Troys, and C. Ampe, *The actin cytoskeleton in normal and pathological cell motility*. Int J Biochem Cell Biol, 2004. **36**(10): p. 1890-909.
10. Li, S., J.-L. Guan, and S. Chien, *BIOCHEMISTRY AND BIOMECHANICS OF CELL MOTILITY*. Annual Review of Biomedical Engineering, 2005. **7**(1): p. 105-150.
11. Quinlan, M.P. and J.L. Hyatt, *Establishment of the circumferential actin filament network is a prerequisite for localization of the cadherin-catenin complex in epithelial cells*. Cell Growth Differ, 1999. **10**(12): p. 839-54.
12. Kovacs, E.M., et al., *Cadherin-directed actin assembly: E-cadherin physically associates with the Arp2/3 complex to direct actin assembly in nascent adhesive contacts*. Curr Biol, 2002. **12**(5): p. 379-82.
13. Goodwin, M. and A.S. Yap, *Classical cadherin adhesion molecules: coordinating cell adhesion, signaling and the cytoskeleton*. Journal of Molecular Histology, 2004. **35**(8 - 9): p. 839-844.
14. Harhaj, N.S. and D.A. Antonetti, *Regulation of tight junctions and loss of barrier function in pathophysiology*. Int J Biochem Cell Biol, 2004. **36**(7): p. 1206-37.
15. Kohler, K. and A. Zahraoui, *Tight junction: a co-ordinator of cell signalling and membrane trafficking*. Biol Cell, 2005. **97**(8): p. 659-65.

16. Van Itallie, C.M. and J.M. Anderson, *The molecular physiology of tight junction pores*. Physiology (Bethesda), 2004. **19**: p. 331-8.
17. Kiuchi-Saishin, Y., et al., *Differential expression patterns of claudins, tight junction membrane proteins, in mouse nephron segments*. J Am Soc Nephrol, 2002. **13**(4): p. 875-86.
18. Harris, T.J. and M. Peifer, *Adherens junction-dependent and -independent steps in the establishment of epithelial cell polarity in Drosophila*. J Cell Biol, 2004. **167**(1): p. 135-47.
19. Nelson, W.J., *Adaptation of core mechanisms to generate cell polarity*. Nature, 2003. **422**(6933): p. 766-74.
20. Bazzoni, G. and E. Dejana, *Endothelial cell-to-cell junctions: molecular organization and role in vascular homeostasis*. Physiol Rev, 2004. **84**(3): p. 869-901.
21. Chiu, Y.J., et al., *Endothelial cell-cell adhesion and mechanosignal transduction*. Endothelium, 2004. **11**(1): p. 59-73.
22. Dejana, E., *Endothelial cell-cell junctions: happy together*. Nat Rev Mol Cell Biol, 2004. **5**(4): p. 261-70.
23. Haigo, S.L., et al., *Shroom induces apical constriction and is required for hingepoint formation during neural tube closure*. Curr Biol, 2003. **13**(24): p. 2125-37.
24. Hildebrand, J.D. and P. Soriano, *Shroom, a PDZ domain-containing actin-binding protein, is required for neural tube morphogenesis in mice*. Cell, 1999. **99**(5): p. 485-97.
25. Dev, K.K., *Making protein interactions druggable: targeting PDZ domains*. Nat Rev Drug Discov, 2004. **3**(12): p. 1047-56.
26. Schiaffino, M.V., et al., *Cloning of a human homologue of the Xenopus laevis APX gene from the ocular albinism type 1 critical region*. Hum Mol Genet, 1995. **4**(3): p. 373-82.
27. Prat, A.G., et al., *Renal epithelial protein (Apx) is an actin cytoskeleton-regulated Na<sup>+</sup> channel*. J Biol Chem, 1996. **271**(30): p. 18045-53.
28. Zuckerman, J.B., et al., *Association of the epithelial sodium channel with Apx and alpha-spectrin in A6 renal epithelial cells*. J Biol Chem, 1999. **274**(33): p. 23286-95.
29. Schild, L., *The epithelial sodium channel: from molecule to disease*. Rev Physiol Biochem Pharmacol, 2004. **151**: p. 93-107.
30. Dietz, M.L., et al., *Differential actin-dependent localization modulates the evolutionarily conserved activity of shroom-family proteins*. J Biol Chem, 2006.
31. Hagens, O., et al., *Disruptions of the novel KIAA1202 gene are associated with X-linked mental retardation*. Hum Genet, 2006. **118**(5): p. 578-90.
32. Seong, K.H., et al., *Application of the gene search system to screen for longevity genes in Drosophila*. Biogerontology, 2001. **2**(3): p. 209-17.
33. Colas, J.F. and G.C. Schoenwolf, *Towards a cellular and molecular understanding of neurulation*. Dev Dyn, 2001. **221**(2): p. 117-45.
34. Copp, A.J., N.D. Greene, and J.N. Murdoch, *The genetic basis of mammalian neurulation*. Nat Rev Genet, 2003. **4**(10): p. 784-93.
35. Greene, N.D. and A.J. Copp, *Mouse models of neural tube defects: investigating preventive mechanisms*. Am J Med Genet C Semin Med Genet, 2005. **135**(1): p. 31-41.
36. Mitchell, L.E., *Epidemiology of neural tube defects*. Am J Med Genet C Semin Med Genet, 2005. **135**(1): p. 88-94.
37. Juriloff, D.M. and M.J. Harris, *Mouse models for neural tube closure defects*. Hum Mol Genet, 2000. **9**(6): p. 993-1000.

38. Doudney, K. and P. Stanier, *Epithelial cell polarity genes are required for neural tube closure*. Am J Med Genet C Semin Med Genet, 2005. **135**(1): p. 42-7.
39. Hildebrand, J.D., *Shroom regulates epithelial cell shape via the apical positioning of an actomyosin network*. J Cell Sci, 2005. **118**(Pt 22): p. 5191-203.
40. Copp, A.J., N.D. Greene, and J.N. Murdoch, *Dishevelled: linking convergent extension with neural tube closure*. Trends Neurosci, 2003. **26**(9): p. 453-5.
41. Wallingford, J.B. and R.M. Harland, *Xenopus Dishevelled signaling regulates both neural and mesodermal convergent extension: parallel forces elongating the body axis*. Development, 2001. **128**(13): p. 2581-92.
42. Schoenwolf, G.C. and J.L. Smith, *Mechanisms of neurulation: traditional viewpoint and recent advances*. Development, 1990. **109**(2): p. 243-70.
43. Zohn, I.E., C.R. Chesnutt, and L. Niswander, *Cell polarity pathways converge and extend to regulate neural tube closure*. Trends Cell Biol, 2003. **13**(9): p. 451-4.
44. Sadler, T.W., *Embryology of neural tube development*. American Journal of Medical Genetics Part C: Seminars in Medical Genetics, 2005. **135C**(1): p. 2-8.
45. Detrick, R.J., D. Dickey, and C.R. Kintner, *The effects of N-cadherin misexpression on morphogenesis in Xenopus embryos*. Neuron, 1990. **4**(4): p. 493-506.
46. Fujimori, T., S. Miyatani, and M. Takeichi, *Ectopic expression of N-cadherin perturbs histogenesis in Xenopus embryos*. Development, 1990. **110**(1): p. 97-104.
47. Lee, J.Y. and B. Goldstein, *Mechanisms of cell positioning during C. elegans gastrulation*. Development, 2003. **130**(2): p. 307-20.
48. Sweeton, D., et al., *Gastrulation in Drosophila: the formation of the ventral furrow and posterior midgut invaginations*. Development, 1991. **112**(3): p. 775-89.
49. Ettensohn, C.A., *Mechanisms of epithelial invagination*. Q Rev Biol, 1985. **60**(3): p. 289-307.
50. Dawes-Hoang, R.E., et al., *folded gastrulation, cell shape change and the control of myosin localization*. Development, 2005. **132**(18): p. 4165-78.
51. Putzke, A.P. and J.H. Rothman, *Gastrulation: PARtaking of the bottle*. Curr Biol, 2003. **13**(6): p. R223-5.
52. Smith, J.L. and G.C. Schoenwolf, *Role of cell-cycle in regulating neuroepithelial cell shape during bending of the chick neural plate*. Cell Tissue Res, 1988. **252**(3): p. 491-500.
53. Lawson, A., J.F. Colas, and G.C. Schoenwolf, *Classification scheme for genes expressed during formation and progression of the avian primitive streak*. Anat Rec, 2001. **262**(2): p. 221-6.
54. O'Rahilly, R. and F. Muller, *The two sites of fusion of the neural folds and the two neuropores in the human embryo*. Teratology, 2002. **65**(4): p. 162-70.
55. Yoder, M. and J.D. Hildebrand, *Shroom4 (KIAA1202) is an actin-associated protein implicated in cytoskeletal organization*. Cell Motil Cytoskeleton, 2006.
56. Ilan, N. and J.A. Madri, *PECAM-1: old friend, new partners*. Curr Opin Cell Biol, 2003. **15**(5): p. 515-24.
57. Newman, P.J. and D.K. Newman, *Signal transduction pathways mediated by PECAM-1: new roles for an old molecule in platelet and vascular cell biology*. Arterioscler Thromb Vasc Biol, 2003. **23**(6): p. 953-64.
58. Jackson, D.E., *The unfolding tale of PECAM-1*. FEBS Lett, 2003. **540**(1-3): p. 7-14.
59. Newman, P.J., *The biology of PECAM-1*. J Clin Invest, 1997. **100**(11 Suppl): p. S25-9.

60. Rossier, B.C., *The epithelial sodium channel: activation by membrane-bound serine proteases*. Proc Am Thorac Soc, 2004. **1**(1): p. 4-9.
61. Morita, K., et al., *Claudin multigene family encoding four-transmembrane domain protein components of tight junction strands*. Proc Natl Acad Sci U S A, 1999. **96**(2): p. 511-6.
62. Rahner, C., L.L. Mitic, and J.M. Anderson, *Heterogeneity in expression and subcellular localization of claudins 2, 3, 4, and 5 in the rat liver, pancreas, and gut*. Gastroenterology, 2001. **120**(2): p. 411-22.
63. Svennevig, K., K. Prydz, and S.O. Kolset, *Proteoglycans in polarized epithelial Madin-Darby canine kidney cells*. Biochem J, 1995. **311** ( Pt 3): p. 881-8.
64. Lavelle, J.P., et al., *Low permeabilities of MDCK cell monolayers: a model barrier epithelium*. Am J Physiol, 1997. **273**(1 Pt 2): p. F67-75.
65. Richardson, J.C., V. Scalera, and N.L. Simmons, *Identification of two strains of MDCK cells which resemble separate nephron tubule segments*. Biochim Biophys Acta, 1981. **673**(1): p. 26-36.
66. Inai, T., J. Kobayashi, and Y. Shibata, *Claudin-1 contributes to the epithelial barrier function in MDCK cells*. Eur J Cell Biol, 1999. **78**(12): p. 849-55.
67. Hildebrand, J.D. and P. Soriano, *Overlapping and unique roles for C-terminal binding protein 1 (CtBP1) and CtBP2 during mouse development*. Mol Cell Biol, 2002. **22**(15): p. 5296-307.
68. Meriane, M., et al., *Cdc42Hs and Rac1 GTPases induce the collapse of the vimentin intermediate filament network*. J Biol Chem, 2000. **275**(42): p. 33046-52.
69. Carenini, S., M. Schachner, and R. Martini, *Cytochalasin D disrupts the restricted localization of N-CAM, but not of LI, at sites of Schwann cell-neurite and Schwann cell-Schwann cell contact in culture*. J Neurocytol, 1998. **27**(6): p. 453-8.
70. Dietz, M.L., et al., *Differential actin-dependent localization modulates the evolutionarily conserved activity of Shroom family proteins*. J Biol Chem, 2006. **281**(29): p. 20542-54.